

Original Article

Solar Interlinking BLDC Motor for Electric Vehicle Charging

Dusa Bhavya¹, A. Raghuram²

^{1,2}Electrical and Electronics Engineering, Jawaharlal Nehru Technological University, Hyderabad, Telangana, India.

¹Corresponding Author : bhavyadusa01@gmail.com

Received: 06 July 2023

Revised: 10 August 2023

Accepted: 03 September 2023

Published: 30 September 2023

Abstract - This paper compares two DC-DC converters to apply electric vehicle charging. The primary supply source is the solar photovoltaic system, whereas the battery is an auxiliary power unit. They power up the BLDC motor. SEPIC and Cuk-SEPIC converters are used for comparative analysis. A control logic has been designed, implementing the regenerative braking logic. With regenerative braking, the energy gets stored in the vehicle battery, by which the vehicle's drive range can be increased. Incremental Conductance MPPT draws the most power from the photovoltaic panel. Switching logic to the gate of the inverter is given to avoid using an additional bi-directional DC-DC converter to reverse current flow during braking action. This reduces the cost, and the efficiency increases. The entire system is implemented in MATLAB/Simulink.

Keywords - BLDC motor, SEPIC converter, Cuk-SEPIC converter, Regenerative braking, Incremental conductance.

1. Introduction

The necessity of renewable energies is emerging significantly, with the extinction of fossil fuels shortly. The availability of renewable energy makes it an advantage to use them as a source of supply. With the rapid growth in the field of power electronics concerning innovation and technology, the application of these renewable energy sources has increased. They are non-exhaustible, and they do not cause any damage to the environment during their usage, though they have few effects in the manufacturing process. Photovoltaic systems use solar energy from the sun as a significant supply source [11, 12]. Various maximum power point techniques have evolved to extract the maximum power from the sun over time. With the extinction of fossil fuels and the current environmental crisis, the evolution of renewable energy sources and the introduction of electric vehicles over Internal Combustion Engine (ICE) vehicles are growing.

An electric vehicle is propelled by an electric motor that receives energy from the battery and can be supplied from a separate source, like solar Photovoltaic system. A significant issue with using electric vehicles is charging stations for the batteries. Moreover, if the size of the battery is increased for a long time, then the cost increases and efficiency decreases. In order to avoid such losses, we can use the energy from regenerative braking. Regenerative brake technology is an energy retrieval method that dips a vehicle moving by transforming its energy from motion (K.E) into something that may be utilized instantly or saved until it is required again. In the proposed system, a solar photovoltaic array will

be interlinked to a BLDC motor via an inverter and DC-DC converter [13, 14]. Maximum power point techniques maximize the output power obtained at SPV terminals. The output DC-DC converter will be fed to a phase VSI, which will feed the BLDC motor. The model that has been suggested is seen in Figure 1. The paper structure is as follows. The introduction part includes the idea and the workflow of the above model. Section II the PV systems and MPP technique are mentioned. SEPIC and Cuk-SEPIC converter designing is seen in section III. Section IV shares a detailed explanation of the proposed system, followed by simulation results and conclusions.

2. Design of Solar Photovoltaic System

In the proposed system, elements like BLDC motor and power electronic switches may account for mechanical, power losses and switching losses, respectively. For this reason, we take the PV array power rating as greater than our requirement, such that it meets the load demand. Table 1 shows the PV array parameters obtained from the PV array block in Simulink. Generally, the voltage at maximum power point is 78% of Open Circuit Voltage (V_{oc}), i.e., $0.78 \times 48 = 37.44$ Volts and the current at maximum power point is 92% of short circuit current, i.e., $0.92 \times 9.36 = 8.71$ A. The BLDC motor we considered has a power rating of 1KW [7]. So, we need to get power per the panel's requirement. If we consider peak sun hours as 5 hours, then the maximum energy extracted by the panel from the sun is $326 \times 5 = 1630$ Wh. If 10% losses are considered, then the total harnessed energy from the sun by solar panel is 1467 Wh.



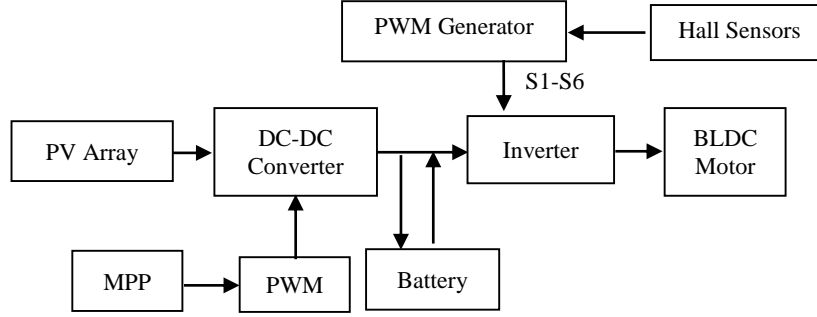


Fig. 1 Block diagram of the proposed system

Table 1. Block parameters of PV array

Module	User-Defined
Maximum Power	326.1024W
Open Circuit Voltage	48V
Short Circuit Current	9.36A
Voltage at MPP	37.44V
Current at MPP	8.71A
Irradiance	1000W/m ²
Temperature	25°C
Series Strings	1
Parallel Strings	1

generator. As seen in Figure 2, at MPP, the gradient is zero, minus to the right, and positive to the left, i.e.

$$\frac{dP_{pv}}{dV_{pv}} = 0; \text{ at MPP}$$

$$\frac{dP_{pv}}{dV_{pv}} > 0; \text{ left at MPP}$$

$$\frac{dP_{pv}}{dV_{pv}} < 0; \text{ right at MPP} \quad (1)$$

Since,

$$\frac{dP_{pv}}{dV_{pv}} = \frac{d(V_{pv} * I_{pv})}{dV_{pv}} = I_{pv} + V_{pv} * \frac{dI_{pv}}{dV_{pv}} \cong I_{pv} + V_{pv} * \frac{\Delta I_{pv}}{\Delta V_{pv}} \quad (2)$$

2.1. Incremental Conductance MPP Technique

The photovoltaic system uses the incremental conductance MPPT technique at its peak power. This technique uses a DC-to-DC converter to regulate the direct duty cycle. The MPP is the point where an incremental conductance ($\Delta I_{pv}/\Delta V_{pv}$) matches the negative of actual conductance (I_{pv}/V_{pv}). The MPPT algorithm regulates the duty cycle, and switching pulses to the converters matching the duty cycle are created using a pulse width modulated

Hence (1) can be written as:

$$\frac{\Delta I_{pv}}{\Delta V_{pv}} = \frac{I_{pv}}{V_{pv}}; \text{ at MPP}$$

$$\frac{\Delta I_{pv}}{\Delta V_{pv}} > - \frac{I_{pv}}{V_{pv}}; \text{ left of MPP}$$

$$\frac{\Delta I_{pv}}{\Delta V_{pv}} < - \frac{I_{pv}}{V_{pv}}; \text{ right of MPP} \quad (3)$$

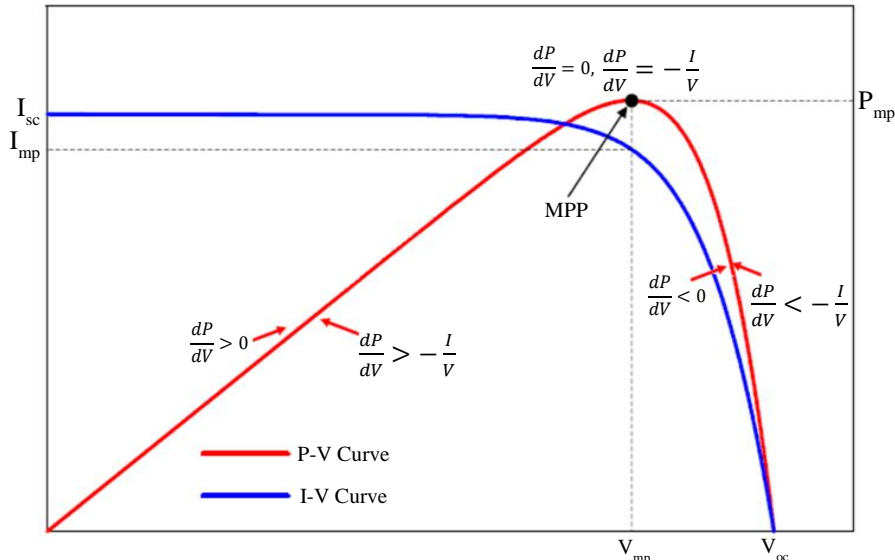


Fig. 2 Power vs Voltage curve of solar panel [1]

```

function D= inc(VA,IA)
persistent VAprev IAprev Dprev
if isempty(VAprev)
    VAprev=0;
end
if isempty(IAprev)
    IAprev=0;
end
if isempty(Dprev)
    Dprev=0.2;
end
D=Dprev;
DeltaVA=VA-VAprev;
DeltaIA=IA-IAprev;
if DeltaVA~=0
    if (DeltaIA/DeltaVA)>(-IA/VA)
        D=Dprev-0.0001;
    elseif(DeltaIA/DeltaVA)<(-IA/VA)
        D=Dprev+0.0001;
    end
elseif DeltaVA==0
    if DeltaIA~=0
        D=Dprev-0.0001;
    end
end
if D>0.9
    D=0.9;
elseif D<0.1
    D=0.1;
end
VAprev=VA;
IAprev=IA;
Dprev=D;
    
```

Fig. 3 Incremental conductance code

The equations from (1) to (3) are taken from [6]. Therefore, from the above relation in equation 3, this technique allows the operating point to move forward (the duty cycle is decreased) if it is on the left of the peak power point and backwards (the duty cycle is increased) if it is on the right side. This increase or decrease stops when the operating point reaches the maximum power point. As the amount of the change decreases, the system controller takes

longer to monitor the MPP of the PV array. To achieve the goals of MPPT and the gentle starting of BLDC motors, the cognitive understanding of recording time and the change in size is maintained. Furthermore, an ideal displacement size ($\Delta D=0.0001$) is chosen, which fosters a gentle beginning and reduces fluctuations near the MPP. The code executed in the MATLAB functional block that illustrates the incremental conductance method is seen in Figure 3.

3. Design of Converters

3.1. SEPIC Converter

The Single-Ended Primary-Inductance Converter (SEPIC) enables the voltage at its output to be higher, lower, or equivalent to the voltage for the device’s input. The regulation of the SEPIC’s output is contingent upon the duty ratio of the control switch (S1). The SEPIC is also called the single-ended primary-inductor converter. The SEPIC converter integrates a variety of features of buck as well as boost converters, thereby enabling a circuit to accommodate variable input voltages while maintaining a consistent output voltage. The SEPIC topology facilitates voltage conversion from one level to another by enabling energy transfer between the capacitive and inductive components. Switch S1, which is commonly a MOSFET transistor, regulates the quantity of energy that is transferred. The expression for the output voltage can be represented as $V_o=V_s*\frac{D}{1-D}$.

SEPIC converter’s circuit diagram is seen in Figure 4. The design parameters of the SEPIC converter are determined by utilizing equations derived from the circuit diagram, which are subsequently implemented in the MATLAB editorial section. The resulting circuit parameters are then utilized in the simulation process. The section of the MATLAB editor where the circuit equations have been executed and the parameters have been derived is seen in Figure 5.

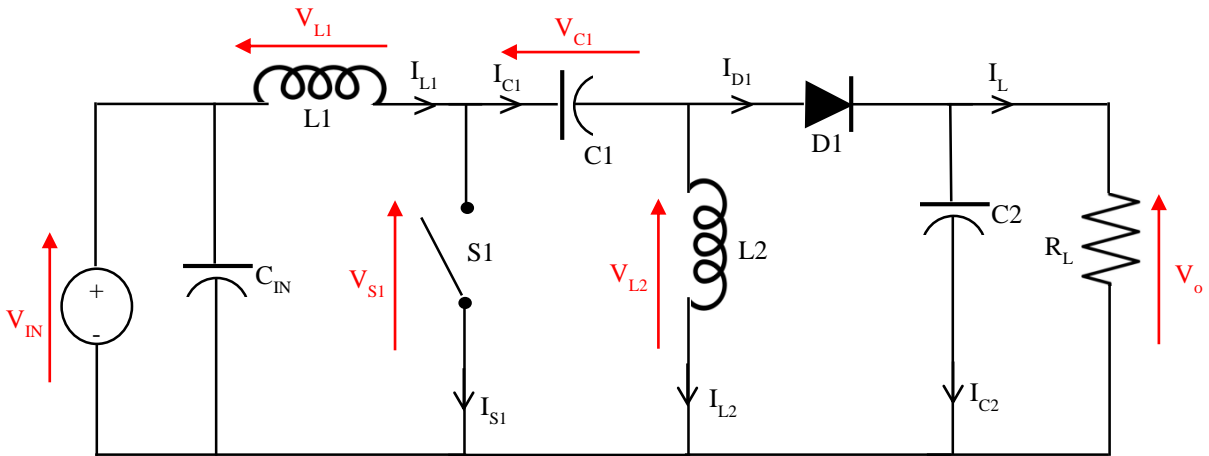


Fig. 4 Circuit diagram of SEPIC converter [2]

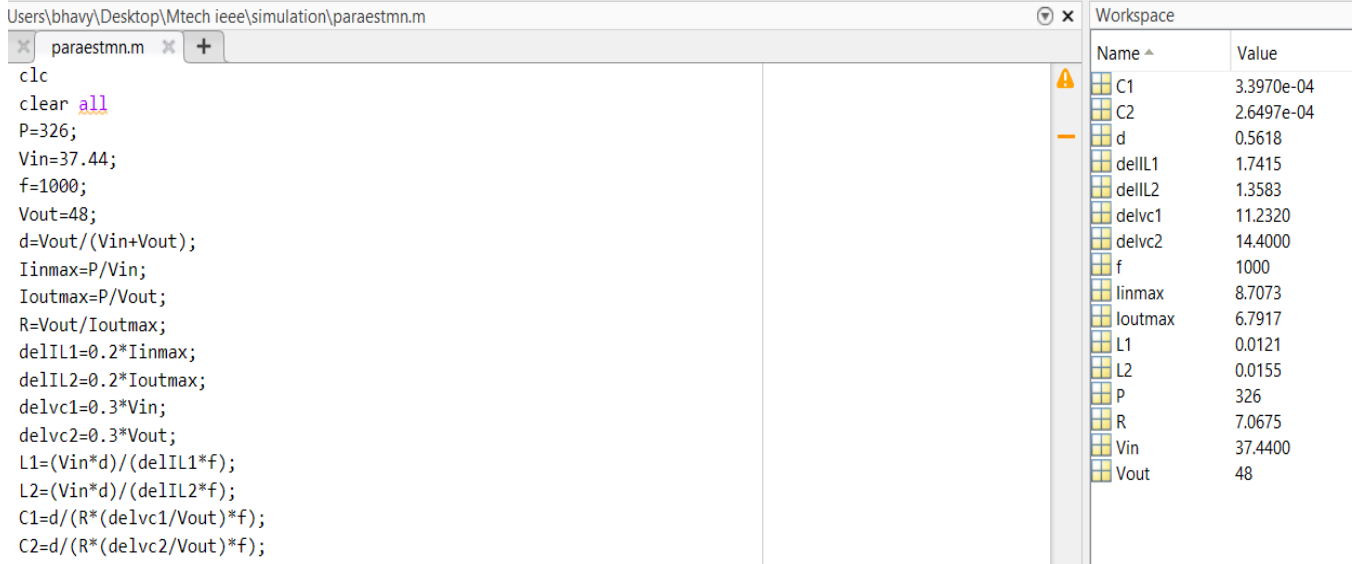


Fig. 5 Circuit parameters of the SEPIC converter

3.1.1.1. Cuk-SEPIC Converter

The Cuk-SEPIC converter is a hybrid of the SEPIC and Cuk converters. These converters share identical voltage conversion ratios, denoted as $(\frac{V_o}{V_{in}})$, and possess an equivalent number of active and passive elements. However, they differ in polarity concerning the common connection point.

The converter is designed with a singular power device to regulate both converters, thereby eliminating the requirement for synchronization with additional switches. The Cuk-SEPIC converter exhibits a more excellent conversion ratio, i.e.,

$\frac{V_o}{V_{in}} = \frac{2D}{D-1}$. A singular switch is utilized to regulate the Cuk and SEPIC converters simultaneously. The SEPIC converter can generate a positive voltage, whereas the Cuk converter can produce a negative voltage. Consequently, the Cuk-SEPIC converter operates in a bipolar manner. The switch facilitates the provision of a congruent ground reference for both positive and negative output voltages. Cuk-SEPIC converter's circuit diagram is seen in Figure 6. Figure 7 depicts the circuit parameters derived from circuit equations formulated and executed within the MATLAB editor section.

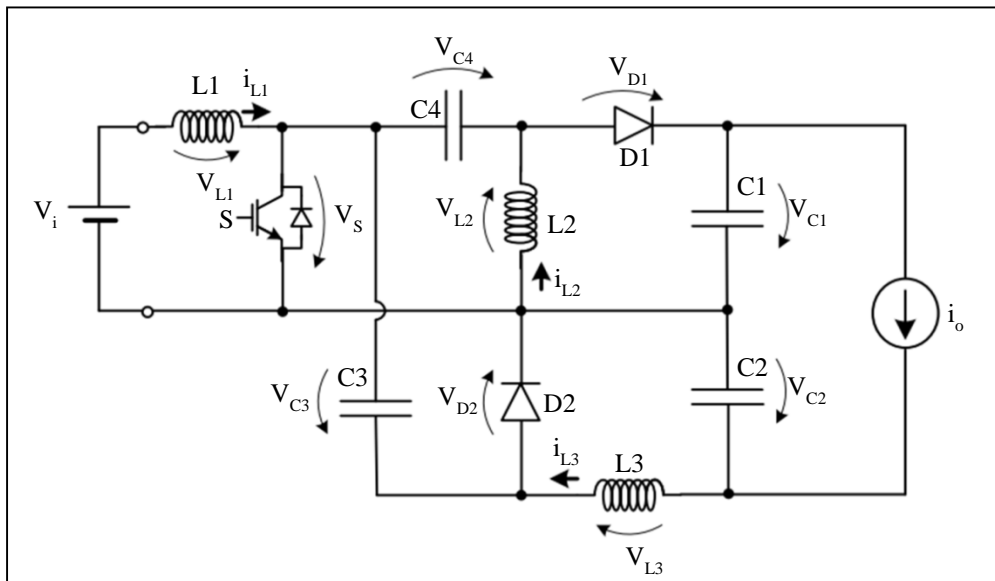


Fig. 6 Circuit diagram of Cuk-SEPIC converter [4]

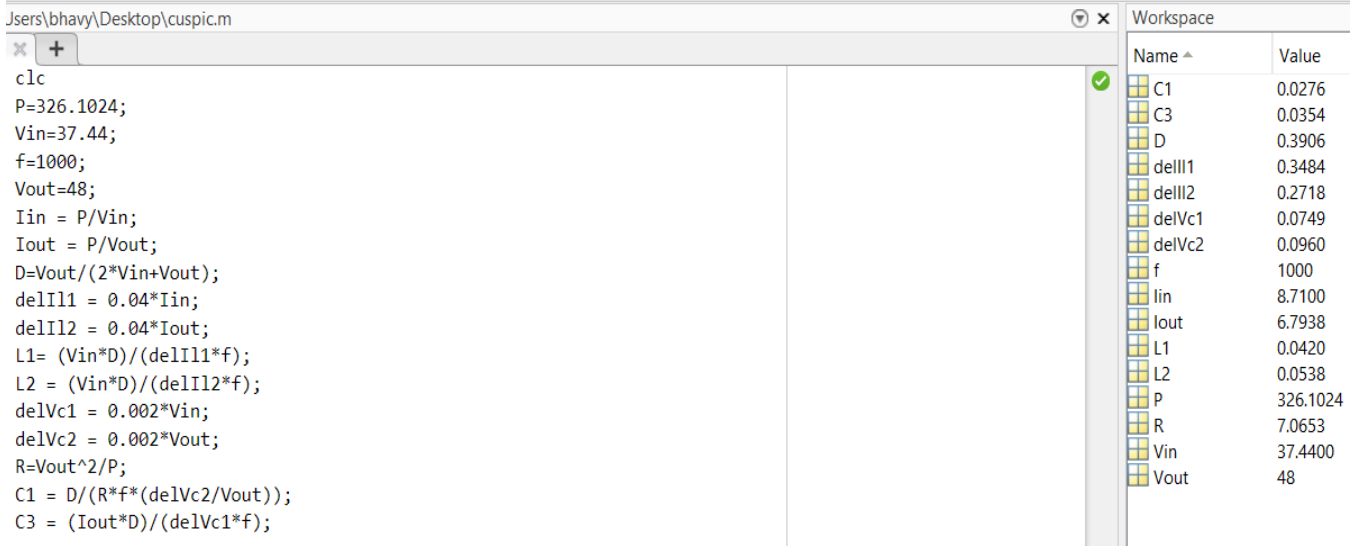


Fig. 7 Circuit parameters of the Cuk-SEPIC converter

4. Proposed System

The Simulink models shown in Figures 8 and 9 were constructed and executed utilizing the MATLAB/Simulink platform. Two distinct DC-DC converters are employed, namely the SEPIC converter, as shown in Figure 8, and the Cuk-SEPIC converter, as shown in Figure 9. The proposed model derives the energy required to overcome frictional forces in the vehicle from a combination of solar panels and batteries. The primary power source is a Photovoltaic (PV)

panel with a power output of 326 watts. The PV panel is subjected to an irradiance of $1000 \frac{W}{m^2}$ and a temperature of $25^{\circ}C$.

The SEPIC converter receives its supply from the PV panel's output. The converter's gating pulse is sourced from the PWM converter used within the system.

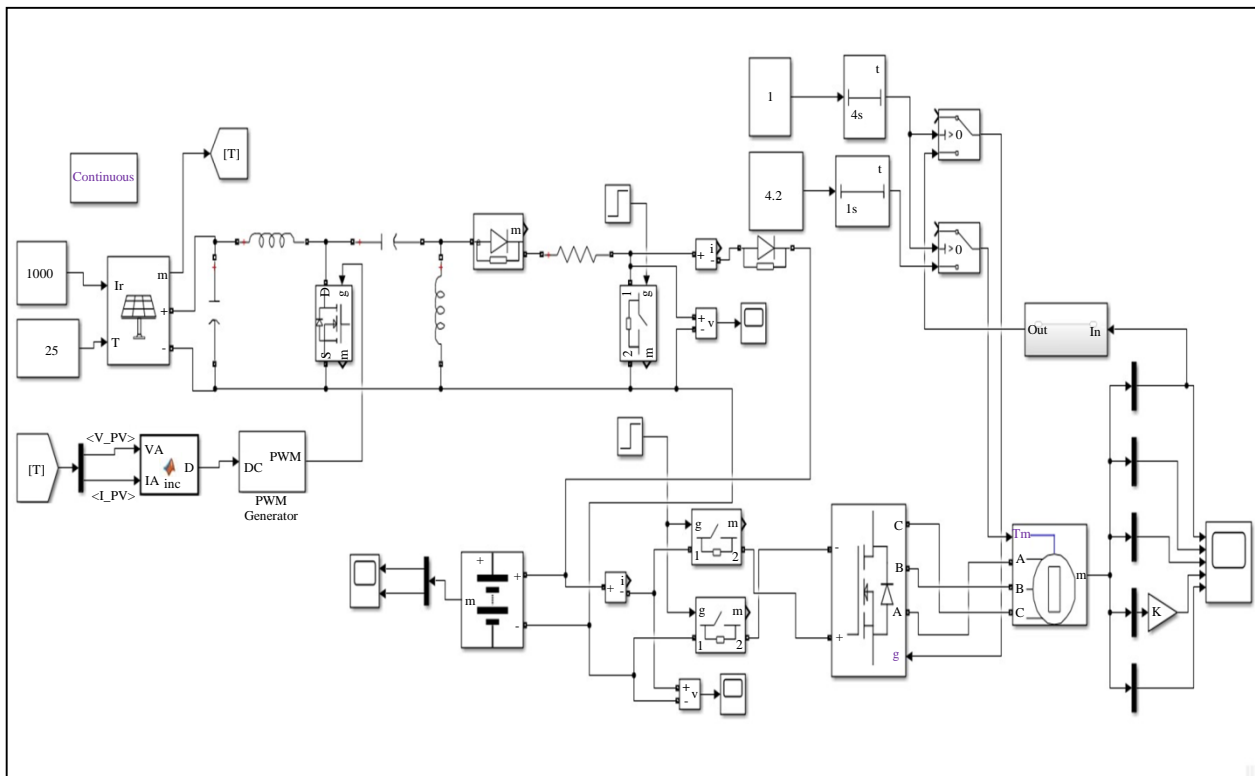


Fig. 8 Simulink model that has been proposed, featuring a SEPIC converter

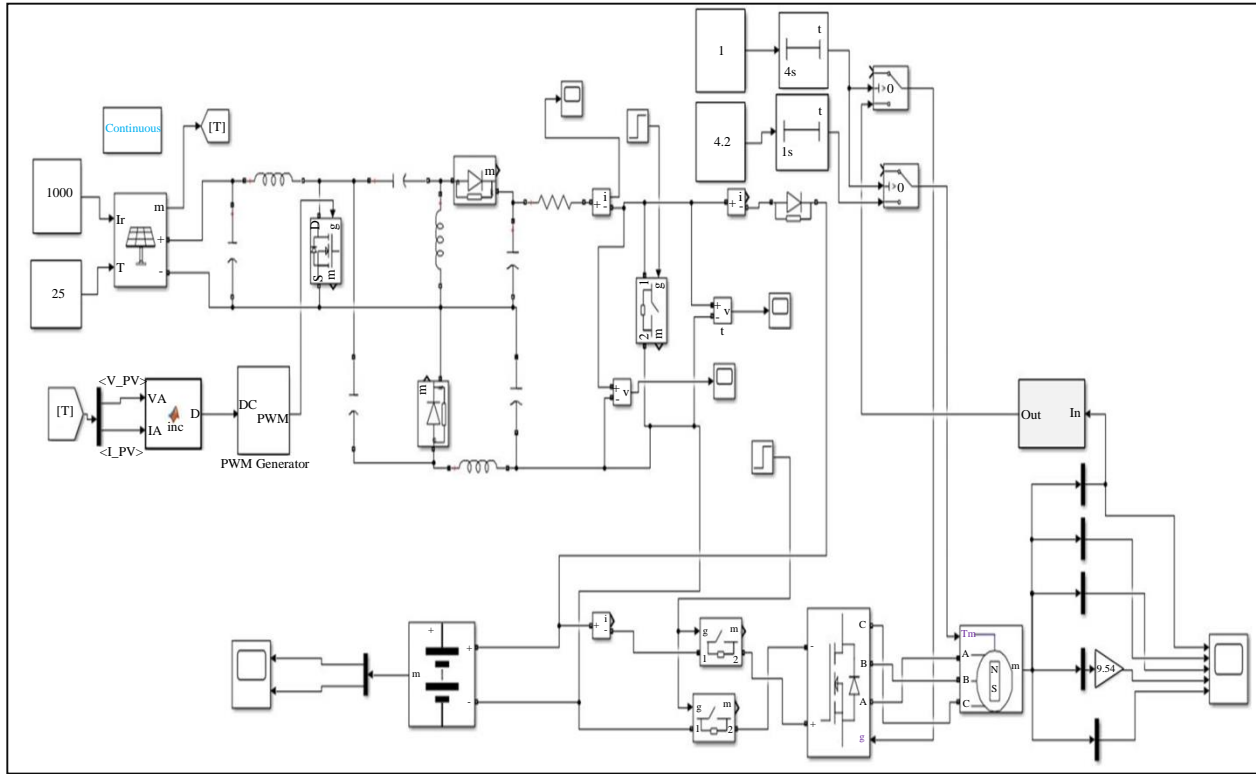


Fig. 9 Simulink model that has been proposed, featuring the Cuk-SEPIC converter

This methodology involves the continuous adjustment of the array terminal voltage following the Maximum Power Point (MPP) voltage, which is determined by the instantaneous and incremental conductance of the Photovoltaic (PV) module [3, 5, 8, 9]. An auxiliary power unit utilizing a Lithium-Ion Battery with a nominal voltage of 48V and a capacity of 100Ah is employed. It is electrically interconnected through the Direct Current (DC) link capacitor. The motor is driven by an AC output generated by a three-phase inverter, which serves as the power input and converts the DC output of the converter.

In order to implement regenerative braking, a circuit was employed to interrupt the signal transmission to the MOSFETs and the torque data transmission to the motor four seconds after commencing the simulation. The control mechanism utilized for the switching process is derived from the hall sensors. The subsystem receives hall signals from a BLDC motor and produces gate signals supplied to the inverter. The design of the switching logic controller is depicted in Figure 10, and the inverter is supplied with gate pulses.

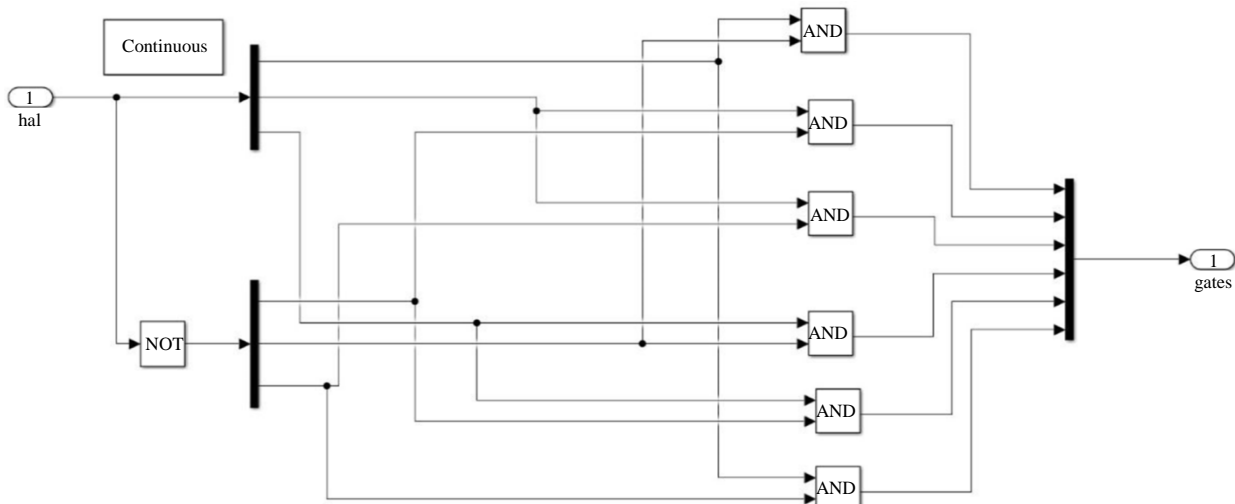


Fig. 10 Controller logic for gate pulses to inverter

During the 0 to 4 seconds, the energized BLDC motor was operating. Regenerative braking was executed after a time interval of 4 seconds. In order to expedite the simulation process, a delay of 1 second was incorporated into the torque data.

During the initial 4-second interval, the motor was provided with torque data and the MOSFETs were subjected to a switching signal. In the fourth second, the switch blocks received a pulse signal to implement the braking logic, and after 4 seconds, slowly, the vehicle started decelerating.

5. Simulation Results

The suggested system is simulated using a SEPIC and a Cuk-SEPIC converter, and the findings are as follows. Figure 11 shows the solar panel’s highest power output with SEPIC and SEPIC-Cuk converter attached, drawing the total power amount. However, the distortion is more significant in the situation of the SEPIC converter. The scope findings in Figure 12 to Figure 15 show the machine’s performance parameters when operated with both converters. They are essentially the same as the machine’s inherent characteristics, irrespective of the type of DC-DC converter employed.

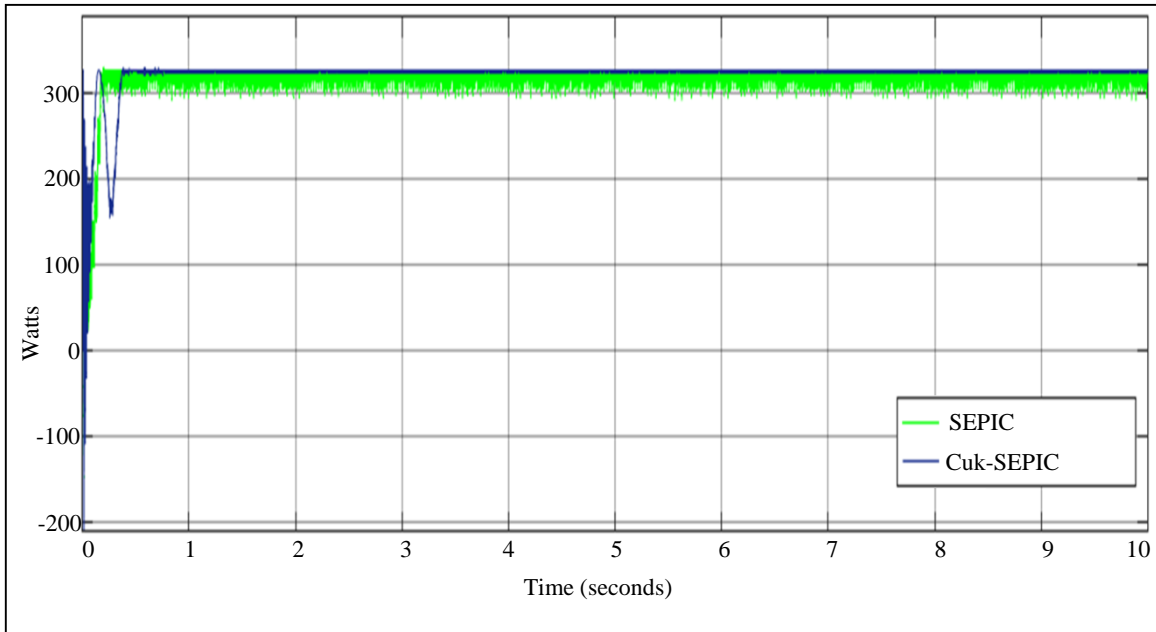


Fig. 11 MPP of the converters

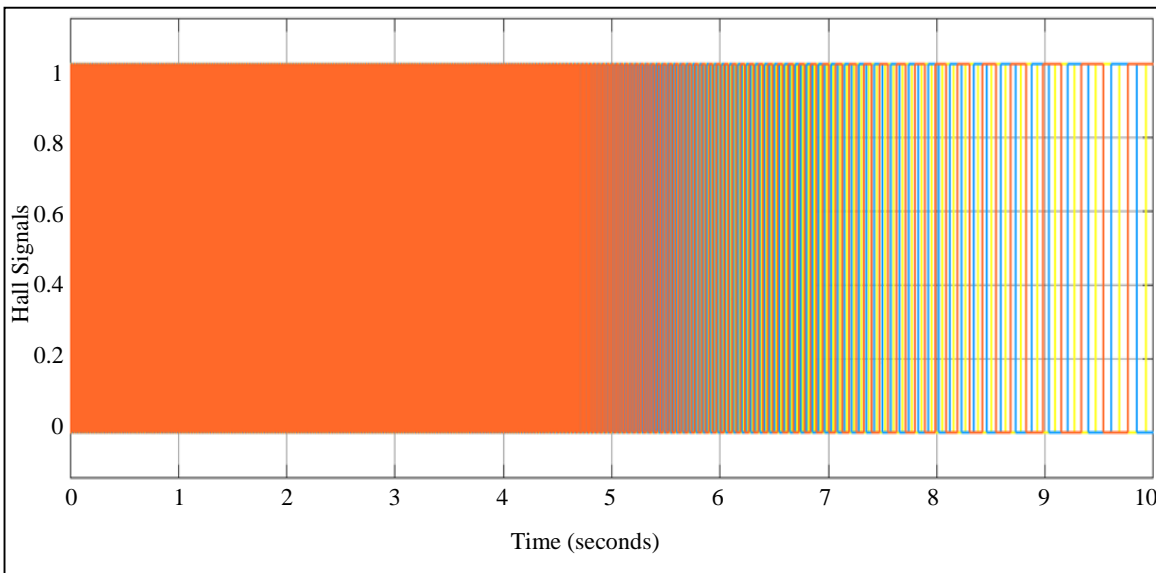


Fig. 12 Hall signals from BLDC motor

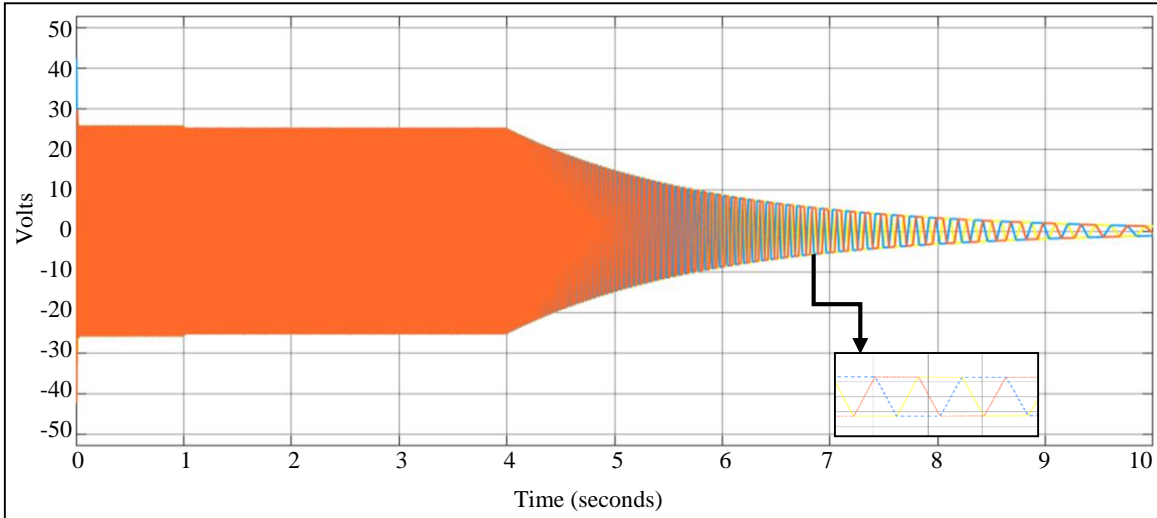


Fig. 13 Back EMF of BLDC motor

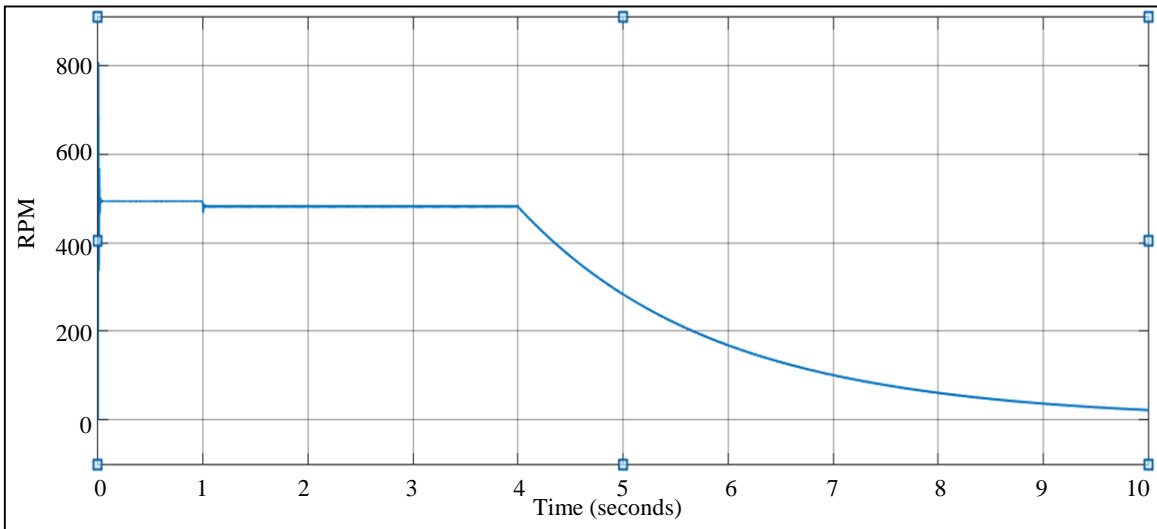


Fig. 14 Speed of BLDC motor

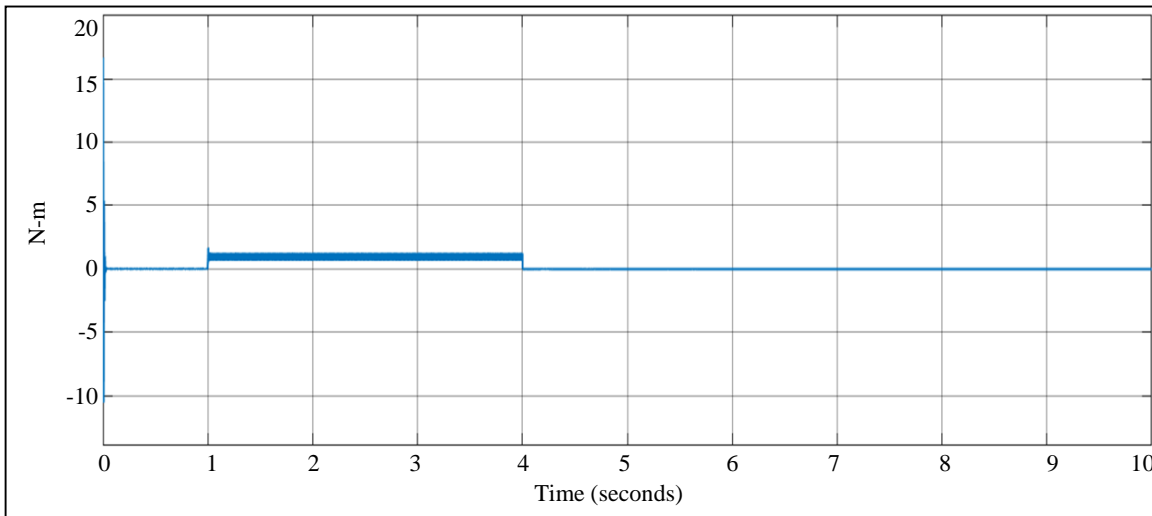


Fig. 15 Torque of BLDC motor

Battery SoC is depicted in Figure 16 and Figure 17, which show a percentage of charging or discharging. The torque information is provided with a 1 second lag to speed up the simulation. In the scenario of a SEPIC converter, the power source and photovoltaic array supply the load for up to 4 seconds. On the other hand, Cuk-SEPIC converter is unique in that it can generate reverse polarity; as a result, the current flows in the opposite direction from the beginning and is charged right away by the solar panel.

At four seconds, the regenerative logic is activated; thus, the current flow goes from the load to the battery. As a result, we observe an increase in battery SoC, which indicates that the battery is charging. Therefore, the energy is being regenerated and stored in the battery. The incoming currents of the two converters are shown in Figure 18, where it is seen that the SEPIC converter experiences more significant oscillations. At the same time, the latter stabilizes after a few transients.

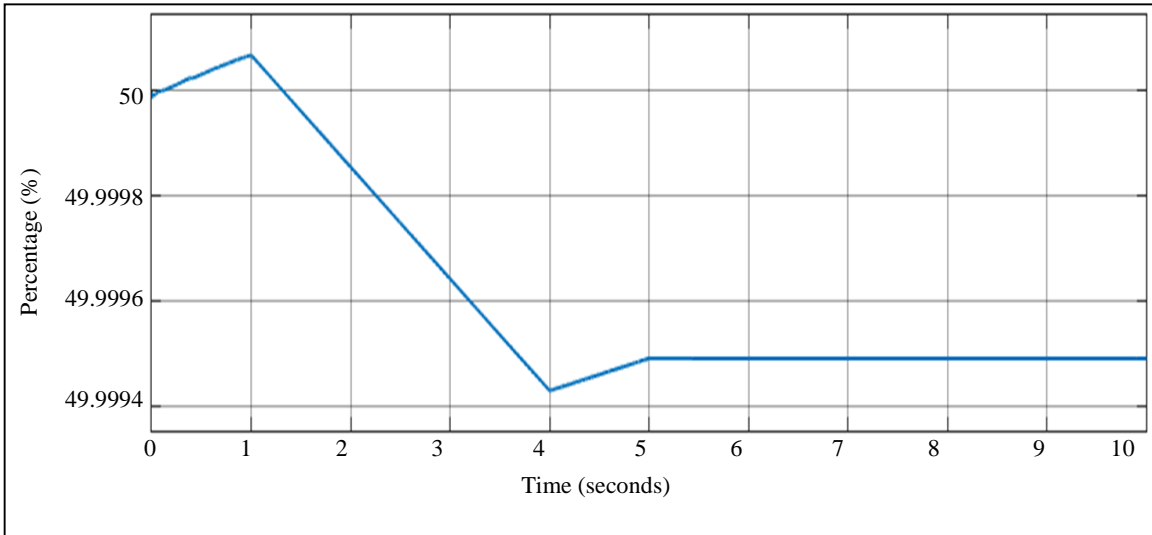


Fig. 16 Battery state of charge with SEPIC converter

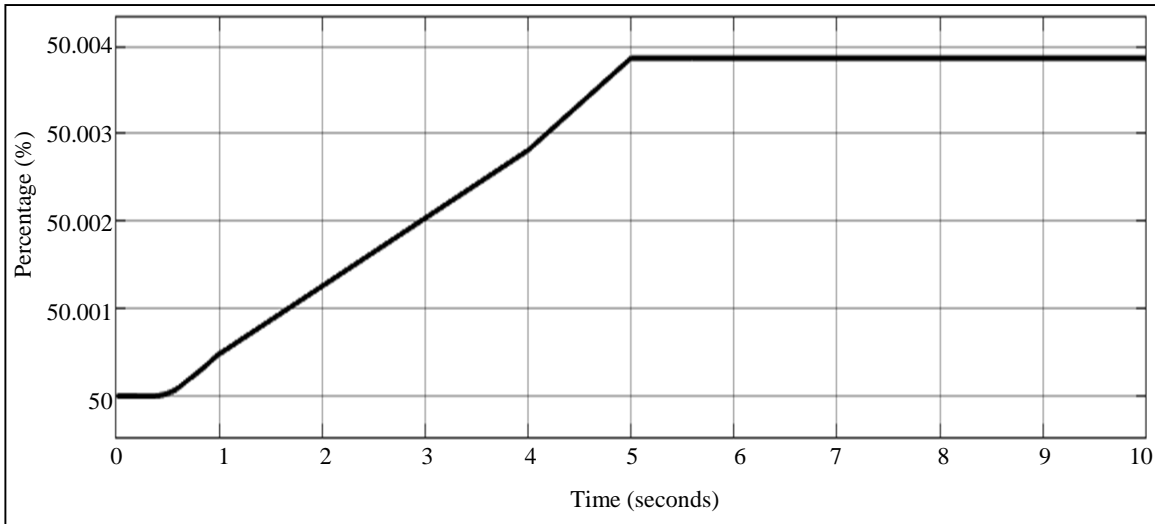


Fig. 17 Battery state of charge with Cuk-SEPIC converter

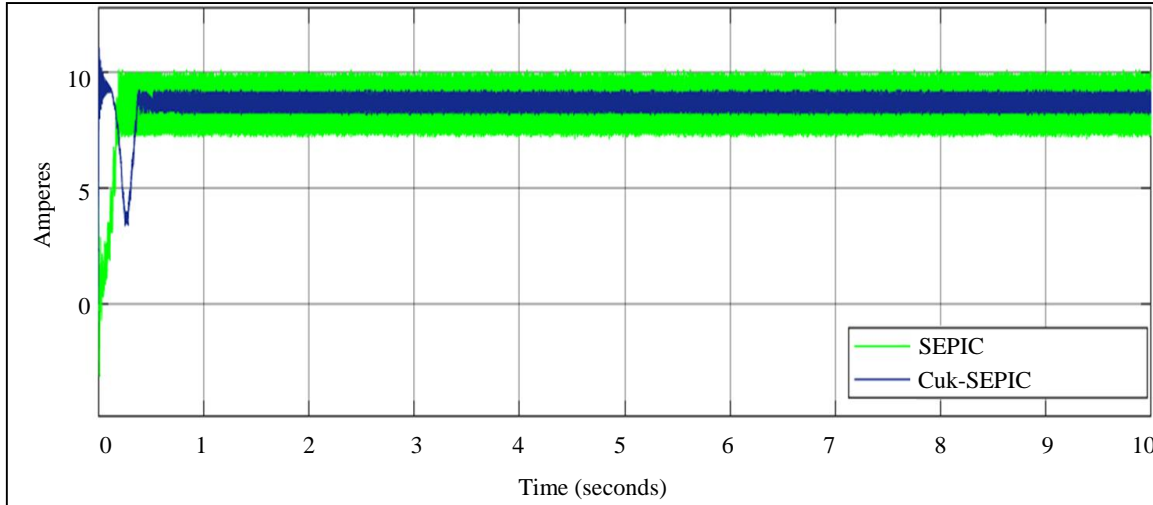


Fig. 18 Input current of converter

6. Conclusion

Based on the simulation results presented, it can be inferred that the Cuk-SEPIC converter exhibits reduced ripple content due to coupling between the input and output inductors. Both converters achieved a maximum power output of 326W using the maximum power point tracking technique. The variations in the SEPIC converter are more significant in magnitude than those observed in the Cuk-SEPIC converter. Therefore, by reducing the input current ripple, the photovoltaic system can be guaranteed to operate close to its maximum power point. When the regenerative braking control logic is engaged in a SEPIC converter, the current flows in a direction opposite to its original direction, resulting

in battery charging. Battery voltage is utilized during the process of motoring in the absence of brake application. In the context of the Cuk-SEPIC converter, it can be observed that the battery is charged from the outset, indicating that the PV system is providing power to both the battery and the load. This happened because of the bipolar voltage characteristic of the Cuk-SEPIC converter, which allows for the flow of current towards the battery from the PV system, resulting in an initial voltage supply to the battery. Upon application of regenerative braking control logic, the battery voltage experiences an increase. Subsequently, upon complete application of the brakes, the battery State of Charge (SoC) stabilizes.

References

- [1] Hala J. El-Khozondar et al., "A Review Study of Photovoltaic Array Maximum Power Tracking Algorithms," *Renewables: Wind, Water, Solar*, vol. 3, no. 1, 2016. [[CrossRef](#)] [[Google Scholar](#)] [[Publisher Link](#)]
- [2] Vijayakumar Gali, and P.B. Amrutha, "Fast Dynamic Response of SEPIC Converter Based Photovoltaic DC Motor Drive for Water Pumping System," *2016 International Conference on Circuit, Power and Computing Technologies (ICCPCT)*, Nagercoil, India, pp. 1-5, 2016. [[CrossRef](#)] [[Google Scholar](#)] [[Publisher Link](#)]
- [3] Yimin Gao, Liping Chen, and Mehrdad Ehsani, "Investigation of the Effectiveness of Regenerative Braking for EV and HEV," *SAE Technical Paper 1999-01-2910*, pp. 1-9, 1999. [[CrossRef](#)] [[Google Scholar](#)] [[Publisher Link](#)]
- [4] P.V. Devika, and Rosemin Parackal, "SEPIC-CUK Converter for PV Application Using Maximum Power Point Tracking Method," *2018 International Conference on Control, Power, Communication and Computing Technologies (ICCPCT)*, Kannur, India, pp. 266-272, 2018. [[CrossRef](#)] [[Google Scholar](#)] [[Publisher Link](#)]
- [5] The IEEE website, 2002. [Online]. Available: <http://www.ieee.org/>
- [6] Bijit Kumar Dey et al., "Mathematical Modelling and Characteristic Analysis of Solar PV Cell," *2016 IEEE 7th Annual Information Technology, Electronics and Mobile Communication Conference (IEMCON)*, Vancouver, BC, Canada, pp. 1-5, 2016. [[CrossRef](#)] [[Google Scholar](#)] [[Publisher Link](#)]
- [7] Adnan Mohammad, and Md. Ziaur Rahman Khan, "BLDC Motor Controller for Regenerative Braking," *2015 International Conference on Electrical Engineering and Information Communication Technology (ICEEICT)*, Savar, Bangladesh, pp. 1-6, 2015. [[CrossRef](#)] [[Google Scholar](#)] [[Publisher Link](#)]
- [8] Yulu Zhang et al., "Design and Simulation Analysis of Anti-Skid Braking System for Mine Electric Locomotive," *International Journal of Recent Engineering Science*, vol. 4, no. 5, pp. 24-28, 2017. [[Google Scholar](#)] [[Publisher Link](#)]

- [9] Roberto F. Coelho, Walbermark M. Dos Santos, and Denizar C. Martins, "Influence of Power Converters on PV Maximum Power Point Tracking Efficiency," *2012 10th IEEE/IAS International Conference on Industry Applications*, Fortaleza, Brazil, pp. 1-8, 2012. [[CrossRef](#)] [[Google Scholar](#)] [[Publisher Link](#)]
- [10] Karim Abdel-Hakam Mohamed, Galal Ali Hassaan, and Adel A. Hegazy, "Induction Motor Electrical Fault Diagnosis by a Fundamental Frequency Amplitude Using Fuzzy Inference System," *International Journal of Recent Engineering Science*, vol. 2, no. 6, pp. 15-24, 2015. [[Google Scholar](#)] [[Publisher Link](#)]
- [11] [Online]. Available: <https://ae-solar.com/read-solar-panel-datasheet/>
- [12] S. Sureshkumar, "Experimental Investigation on Flat Plat Solar Thermoelectric Generator," *International Journal of Recent Engineering Science*, vol. 1, no. 4, pp. 1-5, 2014. [[Google Scholar](#)] [[Publisher Link](#)]
- [13] Stephen Brown, David Pyke, and Paul Steenhof, "Electric Vehicles: The Role and Importance of Standards in an Emerging Market," *Energy Policy*, vol. 38, no. 7, pp. 3797-3806, 2010. [[CrossRef](#)] [[Google Scholar](#)] [[Publisher Link](#)]
- [14] Biswajit Saha, and Bhim Singh, "An Approach for Enhanced Range with Regenerative Braking in Solar PV-Battery Based E-Rickshaw Using Sensorless BLDC Motor Drive," *2020 IEEE International Conference on Computing, Power and Communication Technologies (GUCON)*, Greater Noida, India, pp. 809-814, 2020. [[CrossRef](#)] [[Google Scholar](#)] [[Publisher Link](#)]